Neutron scattering studies of the mechanism of ferroelectricity in $68\%PbMg_{1/3}Nb_{2/3}O_3–32\%PbTiO_3$

2007 J. Phys.: Condens. Matter 19 016219

(http://iopscience.iop.org/0953-8984/19/1/016219)

INSTITUTE OF PHYSICS PUBLISHING JOURNAL OF PHYSICS: CONDENSED MATTER

J. Phys.: Condens. Matter **19** (2007) 016219 (14pp) doi:10.1088/0953-8984/19/1/016219

Neutron scattering studies of the mechanism of ferroelectricity in 68%$PbMg_{1/3}Nb_{2/3}O_3$–32%$PbTiO_3$

S N Gvasaliya[1,2,5], B Roessli[1], R A Cowley[3], S Kojima[4] and S G Lushnikov[2]

[1] Laboratory for Neutron Scattering ETH Zurich and Paul Scherrer Institut, CH-5232, Villigen PSI, Switzerland
[2] Ioffe Physical Technical Institute, 26 Politeknicheskaya, 194021, St Petersburg, Russia
[3] Clarendon Laboratory, Department of Physics, Oxford University, Parks Road, Oxford OX1 3PU, UK
[4] Institute of Materials Science, University of Tsukuba, Tsukuba, Ibaraki 305-8573, Japan

Received 14 November 2006
Published 7 December 2006
Online at stacks.iop.org/JPhysCM/19/016219

Abstract

Neutron scattering has been used to study the relaxor ferroelectric $0.68PbMg_{1/3}Nb_{2/3}O_3$–$0.32PbTiO_3$ (i.e. $(1-x)PbMg_{1/3}Nb_{2/3}O_3$–$xPbTiO_3$ with $x = 0.32$ denoted as 0.68PMN–0.32PT). On cooling, 0.68PMN–0.32PT exhibits a cubic–tetragonal ferroelectric phase transition at $T_c \sim 425$ K. It was found that well above T_c, the transverse optic mode and the transverse acoustic mode are strongly coupled, and a model was used to describe this coupling that gave similar parameters to those obtained for the coupling in $PbMg_{1/3}Nb_{2/3}O_3$ (PMN). At a lower temperature additional quasi-elastic (QE) scattering was found for which the susceptibility follows the temperature dependence of the dielectric susceptibility, as found also in PMN. QE scattering is associated with the dynamic polar nanoregions that occur below the Burns temperature. In addition to QE scattering a strictly elastic central peak (CP) was observed which at wavevectors away from the Bragg peak was much weaker than the CP in pure PMN. On cooling below the ferroelectric phase transition the intensity of the CP decreased. Our results show that the QE scattering and CP observed both in PMN and in the present study result from scattering by dynamic and static nanoregions and can be explained qualitatively by a random-field model.

1. Introduction

The relaxor ferroelectrics have been known for over 50 years but their properties are not yet understood and continue to be the subject of many experiments and theoretical suggestions [1–5]. Much of the effort has been concerned with experiments on either PMN

[5] Author to whom any correspondence should be addressed.

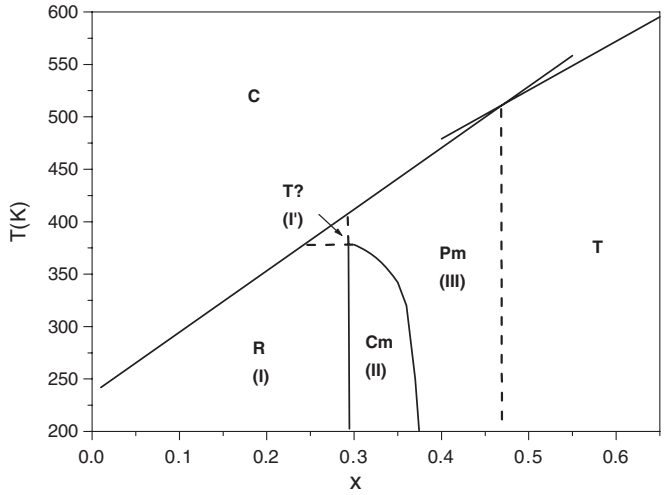

Figure 1. The phase diagram of $(1-x)$PMN$-x$PT showing the symmetries of the different phases. The cubic phase is denoted C, the rhombohedral and tetragonal phases are R and T, and between them are monoclinic phases Cm and Pm, while the symmetry of the phase I' is still uncertain (from [19]).

($PbMg_{1/3}Nb_{2/3}O_3$) or on PZN ($PbZn_{1/3}Nb_{2/3}O_3$) and with these materials doped with PT ($PbTiO_3$). The crystal structure of PMN is cubic in the absence of an applied electric field down to the lowest temperature [6]. Below the Burns temperature, however, which is about 620 K in PMN, optical measurements [7] suggest that the crystal breaks up into polar nanoregions which are locally ferroelectric, while the transverse optic mode at long wavelength becomes over-damped. X-ray and neutron scattering measurements show strong diffuse scattering [6, 8], both quasi-elastic and strictly elastic [9]. In addition, neutron scattering studies indicate that the transverse acoustic (TA) and the lowest transverse optic (TO) branches are coupled [10, 11]. Both Stock *et al* [12] and ourselves [11] have suggested that these properties can be understood in terms of random fields in the cubic crystal. At high temperatures but below the Burns temperature, 620 K, there are dynamic nanoregions produced by the random fields. In this case the random fields have isotropic symmetry and the system cannot develop a long-range ordered structure, as shown by Imry and Ma [13]. At lower temperatures, below 370 K in PMN, the fields develop a cubic anisotropy so that the electric fields are different in the [1, 0, 0] direction from those in the [1, 1, 1] direction, for example. The system then has an increasing number of static nanoregions as the crystal is further cooled. The system has no long-range order except in the presence of an electric field, which is similar to the behaviour found for Ising random fields in magnetic systems [14].

Lead titanate, PT, is a more conventional ferroelectric crystal with a soft mode and a transition to a long-range ordered structure occurring below 770 K [15]. The low-temperature phase is tetragonal and similar to that occurring in ferroelectric $BaTiO_3$ just below its Curie point. Mixed crystals can be grown for all concentrations $1-x$ of PMN and x of PT. The phase diagram has been measured in detail [16–20] and is shown in figure 1. For small x, small amounts of PT, there is a transition to a long-range ordered ferroelectric state with rhombohedral symmetry, although as commented above this transition does not occur in pure PMN. As the concentration x is increased to about 0.32, the ferroelectric transition temperature increases from around 250 K for x about 0.1 to about 400 K for $x \sim 0.32$. There is some

evidence of distortions from the rhombohedral structure, for $x > 0.28$, but, by and large, the structure of this phase is clear. When the concentration of PMN is above $x = 0.5$, the transition temperature rises and reaches 770 K for $x = 1$, and the long-range ordered ferroelectric phase occurring below the transition temperature is tetragonal. Between the rhombohedral phase and the tetragonal phase the measurements are difficult because these are often made with thin films and the effect of strains from the substrates and weak electric fields can be considerable. Nevertheless, the structure has been determined as monoclinic, while the birefringence measurements suggest that there is a first-order transition between a phase with Cm symmetry and one with Pm symmetry. Both of these phases seem to have continuous phase transitions to the rhombohedral and tetragonal phases respectively.

The structure of these phases can be understood qualitatively by using the Landau theory of phase transitions. The free energy is expanded in powers of the spontaneous polarization $\mathbf{P} = (P_x, P_y, P_z)$ as [21]

$$F = A(T - T_c)P^2 + BP^4 + C(P_x^4 + P_y^4 + P_z^4) + \cdots \tag{1}$$

where the ferroelectric transition occurs when $T = T_c$ and A, B, and C are constants. The first two terms in this expansion are isotropic terms and so do not influence the direction of the spontaneous polarization. The third term describes the cubic anisotropy and in conventional ferroelectrics the direction of the polarization is dependent on the sign of the coefficient C or in some cases on higher-order terms. Low-order perturbation theory shows that if $B > 0$ and C is positive the minimum of the free energy occurs if the spontaneous polarization is along a [1, 1, 1] direction giving a rhombohedral structure, while if C is negative the minimum occurs when the polarization is along the [1, 0, 0] direction giving a tetragonal structure. It is then natural to describe the phase diagram of PMN–PT by assuming that C is positive for $x < 0.32$ and negative for $x > 0.32$, at least close to the onset of ferroelectricity. Of course in these diffuse ferroelectrics the properties are more complicated because the random electric fields introduce disorder into the free energy and higher-order terms in the expansion of the free energy can result in transitions to a monoclinic phase as described by Vanderbilt and Cohen [22].

Although there have been many studies of the structure of the mixed crystals there have been very few measurements of the dynamical properties and of the phonon spectra. Recently there has been a neutron and x-ray scattering study by Stock *et al* [23] of samples with $x = 0.6$, well into the tetragonal part of the phase diagram. The results showed that the diffuse scattering was absent or at least much weaker in this sample than in PMN, and it was suggested that the polar nanoregions found in relaxor ferroelectrics were not present. Nevertheless aspects of the scattering, such as the waterfall effect, were observed and interpreted as arising from random fields. Earlier work by Koo *et al* [24] studied a sample having $x = 0.2$ that corresponds to the rhombohedral part of the phase diagram. This experiment was performed before it was realized that it is important to separate out and describe the quasi-elastic and central peak scattering [9]. Nevertheless the diffuse scattering in this crystal was found to be intense and temperature dependent. However, recent work has shown that the determination of the quasi-elastic scattering components is important and can only be made if cold neutrons are used to give the high resolution required. In both of these earlier studies thermal neutrons were used, which do not offer a sufficiently high-energy resolution to separate the diffuse scattering into a strictly elastic and a quasi-elastic component as is now seen to be important, for example in PMN [9, 11].

In this paper we report on high-resolution cold-neutron scattering measurements on a sample with $x = 0.32$ close to the concentration where the averaged cubic anisotropy is expected to be very small. The materials are useful for piezoelectric applications because the ordered ferroelectric moments can be rotated very easily by applying stresses to the materials

and as a result the piezoelectric constants are unusually large and have technological uses. The measurements were performed with a similar configuration to that used to study the dynamical properties of PMN [11]. The details of the sample and of the resolution of the neutron spectrometer are given in section 2. In section 3 we describe the measurements made and, as also found in PMN, there is a strong coupling between the transverse optic mode and transverse acoustic mode. In a final section we discuss our results and compare them with the results on PMN and with those obtained by Stock *et al* with $x = 0.6$ [23].

2. Experimental details

A high-quality crystal of 0.68PMN–0.32PT was grown by TRS Ceramics. The mosaic spread is less than 0.5°. The sample, of cubic shape with a size of 1 cm^3, was aligned in the (hhl) scattering plane and placed in a niobium holder which could be mounted inside a furnace.

The measurements were performed with the TASP [25] triple-axis spectrometer located at the spallation neutron source, SINQ [26], of the Paul Scherrer Institut in Switzerland. The spectrometer was configured with both a pyrolytic graphite (PG) monochromator and analyser and operated so that the scattered energy was held constant. For most of the experiments the collimation from source to detector was 0.63°–0.67°–0.67°–1.33° horizontally and the final scattered wavelength was 3.83 Å. A PG filter was used in the scattered beam to eliminate higher-order neutrons. The energy resolution at zero energy transfer was 0.2 meV, FWHM, and the wavevector resolution was approximately 0.012, 0.015 and 0.1 $Å^{-1}$ parallel to the scattering vector, perpendicular but in the horizontal plane, and vertically, respectively.

Most of the data were obtained by scanning the spectrometer so that:

(a) the energy or wavevector was held constant in either the (1, 1, 0) or (2, 2, 0) Brillouin zones while the temperature was set at 700 K;
(b) the wavevector or energy was held constant in the (1, 1, 0) Brillouin zone while the temperature was kept at either 430 or 475 K;
(c) the wavevector was held constant at either (1, 1, 0.75) or (2, 2, 0.75) while the temperature was varied between 330 and 700 K.

In this description, and henceforth in this paper, the wavevector transfers are given in reciprocal lattice units (rlu), $2\pi/a$.

3. Experimental results

3.1. Phase transitions

The Bragg scattering from the structure of the sample of 0.68PMN–0.32PT was measured so as to determine whether it was consistent with the phase diagram given in figure 1. The results for the temperature dependence of the scattering from the (002) Bragg peak are shown in figure 2. There is a change in the slope of the curve at about 425 K which agrees with the temperature of the continuous transition to the ferroelectric phase with a structure which is possibly tetragonal. There is then a rapid increase in the intensity between 370 and 380 K which is consistent with the transition from the Pm phase to the Cm phase and is possibly of first order although slightly smeared by any concentration gradient across the crystal. The temperatures are slightly larger than those found by Shuvaeva *et al* [19], but this may be due to the different origin of the samples.

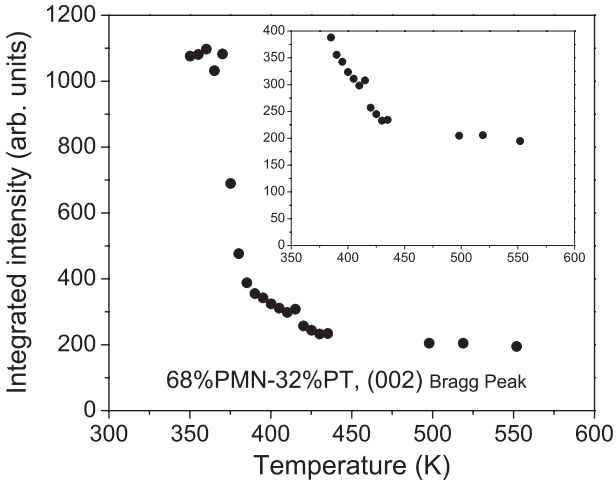

Figure 2. The temperature dependence of the integrated intensity of the (002) Bragg peak of a 0.68PMN–0.32PT single crystal. Structural phase transitions can be identified for temperatures of 425 and 375 K.

3.2. Measurements at 700 K

The neutron scattering was measured near the (1, 1, 0) and (2, 2, 0) reciprocal lattice points. As shown in figure 3, the inelastic scattering near the (1, 1, 0) lattice point was dominated by the transverse acoustic mode with only a small amount of scattering that could be ascribed to the transverse optic mode. Because of this the structure factor of the TO phonon in the (1, 1, 0) zone was fixed to zero for the fits. The relative intensity of the inelastic scattering steadily decreases compared with the elastic scattering as the wavevector transfer increases. In contrast near the (2, 2, 0) reciprocal lattice point the transverse optic mode has the larger intensity, as shown in figure 4, which shows the results for both constant wavevector scans and for constant energy scans.

These results are similar to those for PMN at high temperatures and show that there is no quasi-elastic scattering at 700 K in 0.68PMN–0.32PT. In PMN we found [11] that the QE scattering appears at the Burns temperature. Consistently with these results we can assume that the temperature $T = 700$ K of 0.68PMN–0.32PT is above the Burns temperature. Unfortunately we are not aware of any determination of the Burns temperature in the doped material. When the Burns temperature is assumed to vary linearly between the Burns temperature for PMN and the ferroelectric temperature for PT as in [24] the result is consistent with our results. The scattering profiles have been fitted to two coupled modes for each scan. Using the same notation as previously [11], the energy of the transverse acoustic mode was parameterized as

$$\omega_{\mathrm{TA}} = d \sin(\pi q) \tag{2}$$

and the energy of the transverse optic mode as

$$\omega_{\mathrm{TO}}^2 = \omega_0^2 + c \sin^2(\pi q) \tag{3}$$

with the coupling between the two modes having the form

$$\Delta = \Delta_{12} \sin^2(\pi q). \tag{4}$$

The damping of the transverse acoustic mode is given by

$$\gamma_{\mathrm{TA}} = D_{\mathrm{TA}} \sin^2(\pi q) \tag{5}$$

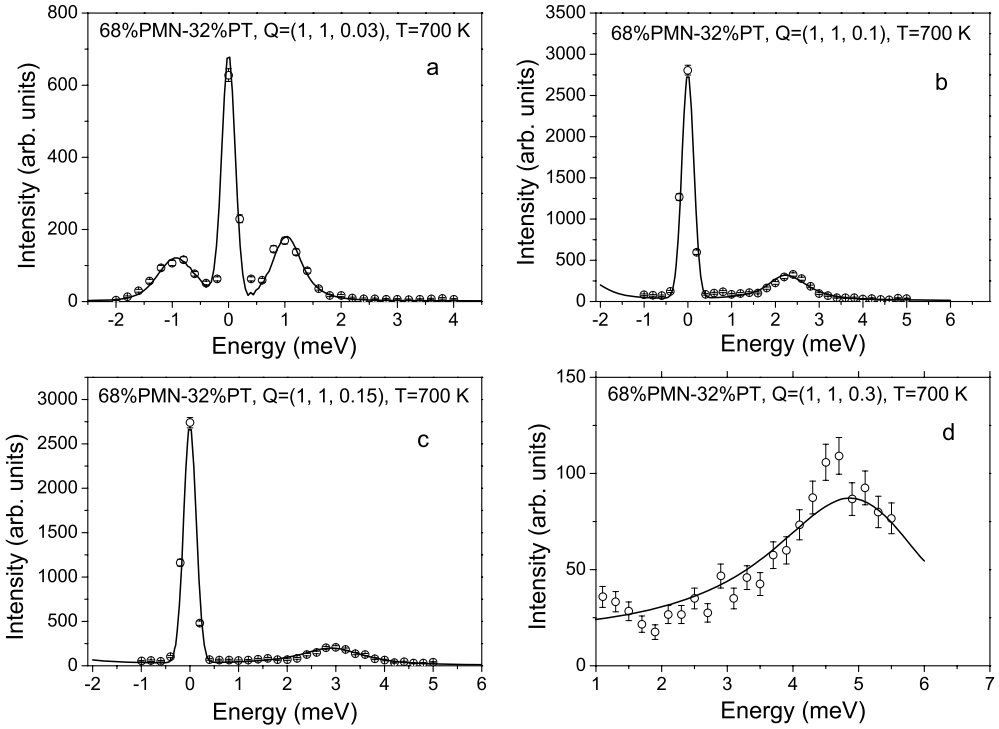

Figure 3. Representative constant Q scans in the vicinity of the (1, 1, 0) Bragg peak at a temperature of 700 K. The fits are described in the text and shown by solid lines.

while for the optic mode the damping was chosen for each wavevector. The coupled-mode model was used to calculate the susceptibility and then the neutron scattering cross section as described in our earlier paper on PMN [11]. The parameters were fitted to the experimental results and the energies of the modes are shown in figure 5 with the parameters $d = 11.4 \pm 0.4$ meV, $\omega_0 = 2.7 \pm 0.2$ meV, and $c = 165.4 \pm 9.8$ meV^2. The coupling between the modes is given by $\Delta_{12} = 117.3 \pm 4.1$ meV^2. These are slightly larger than the parameters in PMN with the increase varying between 28% for Δ_{12} and 12% for d. The value of the imaginary part of the coupling term was found to be similar to PMN and was fixed at the value $\gamma_{12} = 1.5$ meV. The damping of the transverse optic and transverse acoustic modes are shown in figure 6. The results for the transverse acoustic mode are a smooth curve with $D_{\mathrm{TA}} = 3.5 \pm 0.2$ meV. This value is lower by 17% than the value of the damping observed in PMN. The damping of the transverse optic mode shows considerable scatter but has an average value that is about 1.5 meV. The indication is that the transverse optic mode at the zone centre does not completely soften as found in most other relaxor ferroelectrics.

3.3. The temperature dependence of the spectrum and quasi-elastic scattering

The neutron scattering at wavevector transfers of (1, 1, 0.075) and (2, 2, 0.075) was measured at a range of temperatures between 330 and 700 K, as shown in figure 7. Fits were made using the coupled-phonon model described in the previous section, with the addition of both a quasi-elastic peak and a strictly elastic peak. There was little change in the parameters, as shown in figure 8 for the dispersion and structure factor of the transverse acoustic mode.

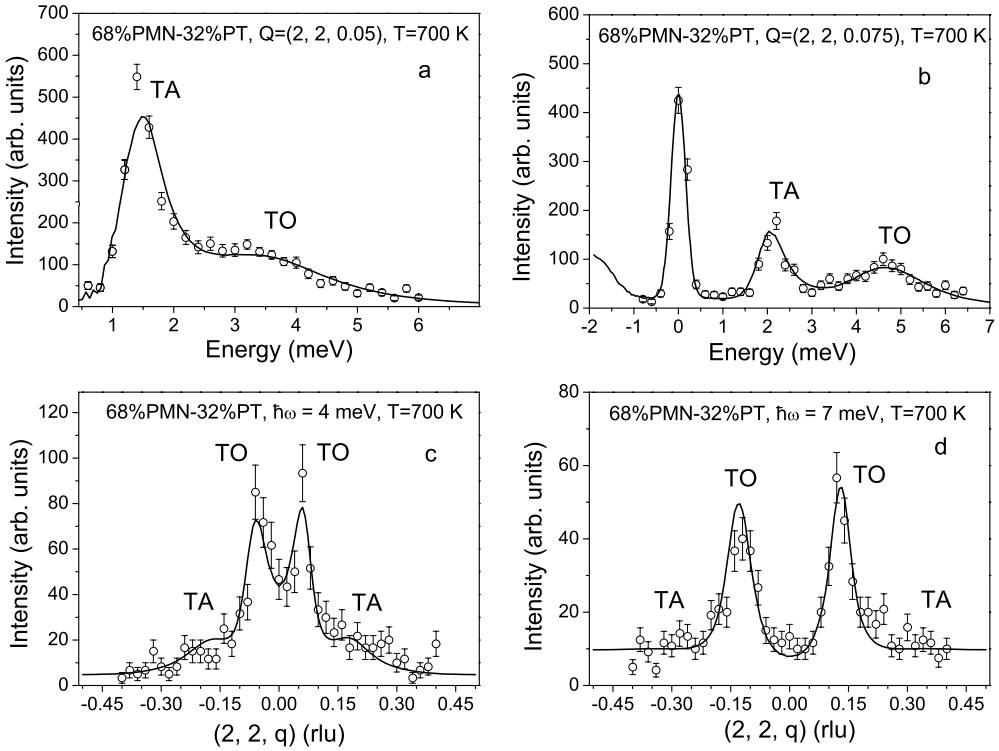

Figure 4. Representative constant Q scans and constant energy scans with $E = 4$ and 7 meV, in the vicinity of the (220) Bragg peak at a temperature of 700 K. The solid lines are the results of fits that are described in the text.

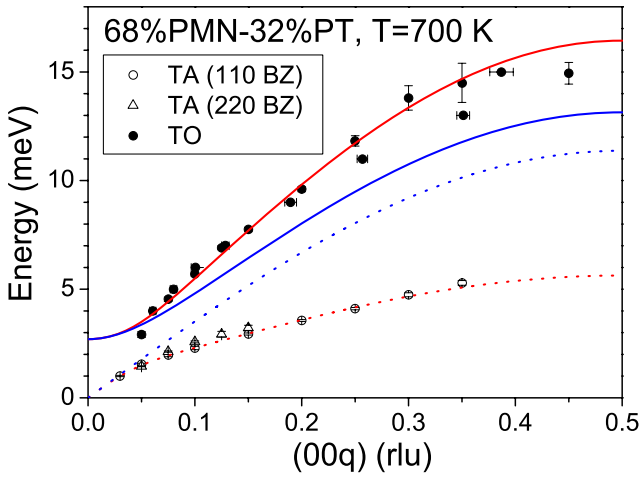

Figure 5. The dispersion curves for the TO and TA phonons propagating along the [001] direction. The two inner curves give the uncoupled energies of the modes while the outer two curves give the energies of the coupled modes.

(This figure is in colour only in the electronic version)

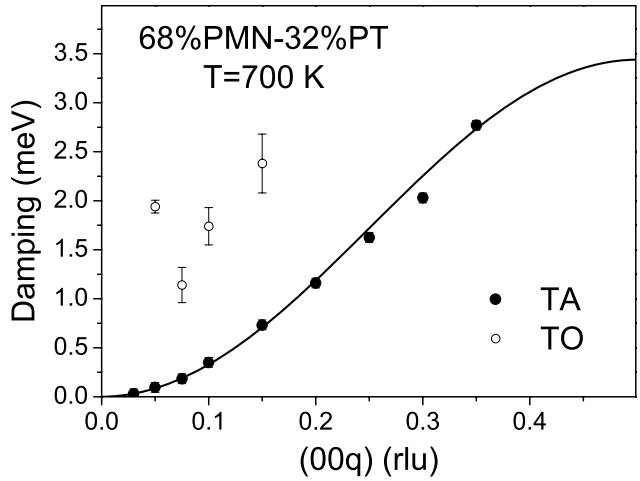

Figure 6. The results of the fitting for the damping of the TA and TO modes from constant Q scans. The TA mode is given by the smooth curve and the open points the damping of the optic mode.

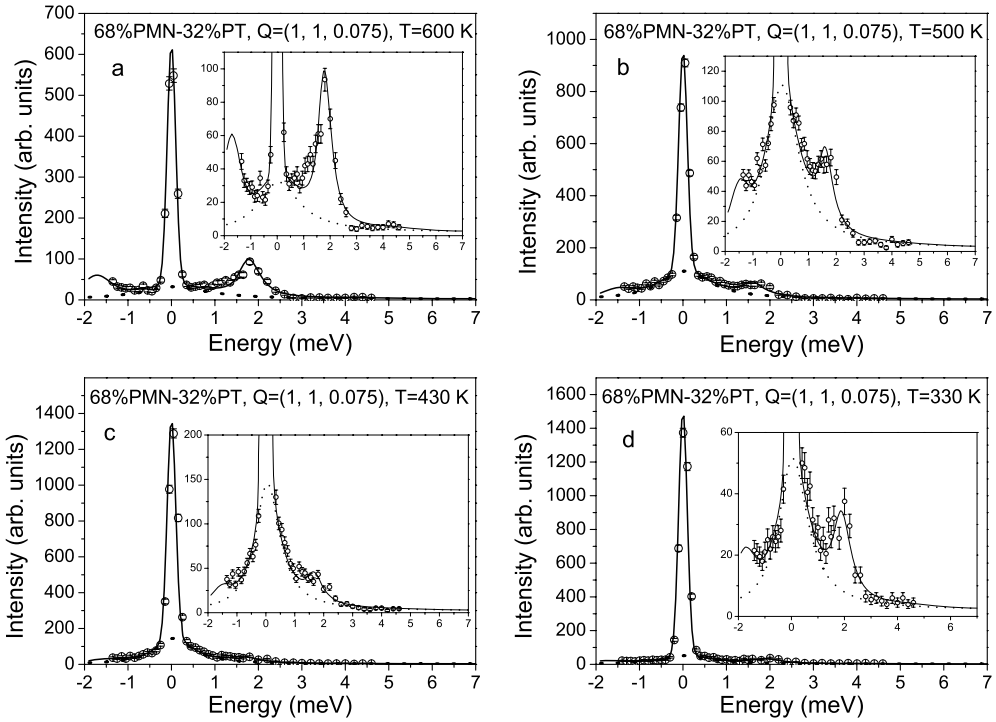

Figure 7. The temperature dependence of the intensity obtained from experiments in which the wavevector transfer was held fixed at (1, 1, 0.075). The fits are described in the text.

Both decreased on cooling from 700 K to about 450 K and then increased slightly as the temperature was further cooled. The broad minimum in the curves as a function of temperature is, within error, consistent with the temperature of the ferroelectric phase transition. Note that

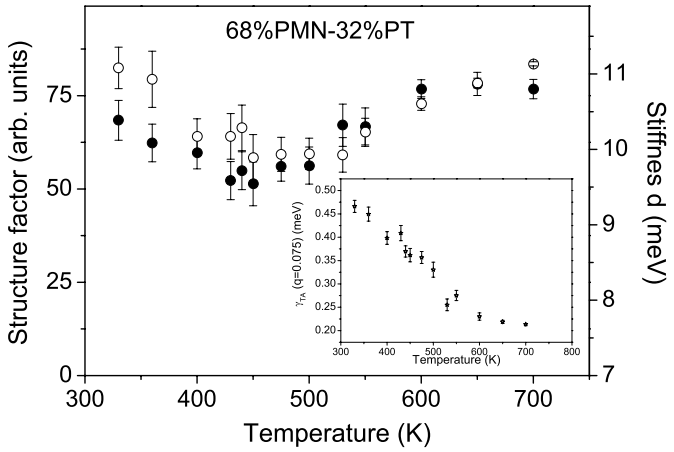

Figure 8. The temperature dependence of the slope (stiffness) shown by the open circles and structure factor of the TA mode shown by the solid circles as measured near the (1, 1, 0) Bragg reflection. Note that the corresponding values obtained directly from data taken near the (2, 2, 0) Bragg reflection show temperature-independent behaviour while the fractional changes for the (1, 1, 0.075) data are also small. The inset shows the temperature dependence of the damping of the TA mode as obtained from the data taken at $Q = (1, 1, 0.075)$.

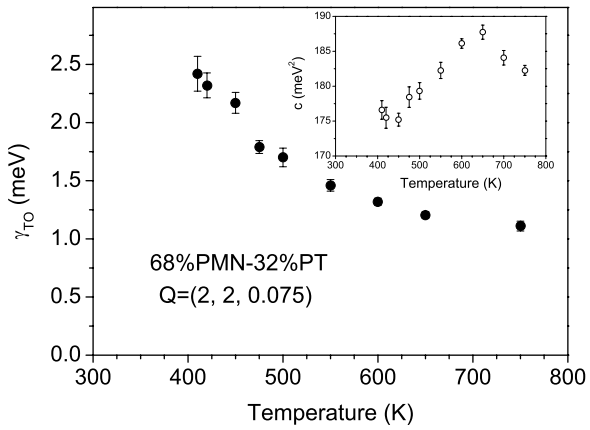

Figure 9. The temperature dependence of the damping of the TO phonon as measured near the (2, 2, 0) Bragg reflection. The inset shows the temperature dependence of the stiffness c of the TO phonon as deduced from the data at the (2, 2, 0.075) position with $\omega_{TO}(0)$ kept fixed for the fits.

the corresponding values obtained directly from data taken near the (2, 2, 0) Bragg reflection show temperature-independent behaviour. The damping of the TO phonon increases gradually on approaching the phase transition, as shown in figure 9.

There is, however, considerable change in the scattering in the region around the elastic peak. As shown in figure 7, on cooling from 700 to 320 K there is a broad maximum in the quasi-elastic scattering centred on 430 K, as illustrated in figure 10. Also shown in figure 10 is the temperature dependence of the dielectric susceptibility, which has a similar peak, although the latter is considerably sharper than the neutron scattering measurements. Possibly this is because the quasi-elastic scattering is measured at a non-zero value of the wavevector transfer, namely (1, 1, 0.075), while the dielectric susceptibility is not. Similar

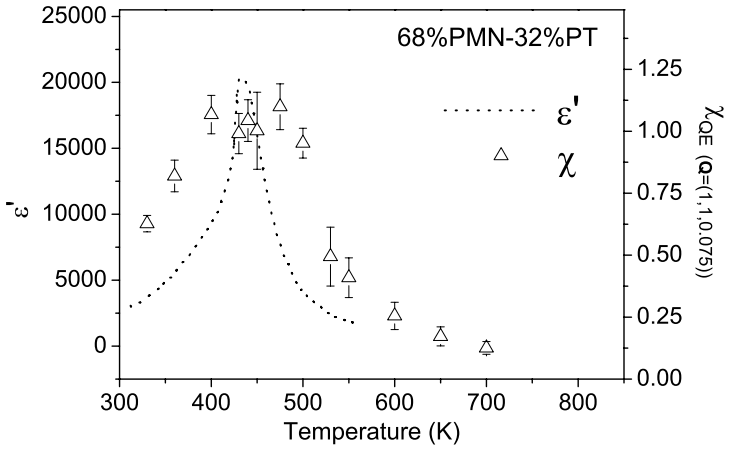

Figure 10. The temperature dependence of the susceptibility of the quasi-elastic scattering as measured at (1, 1, 0.075) compared with the dielectric susceptibility [20].

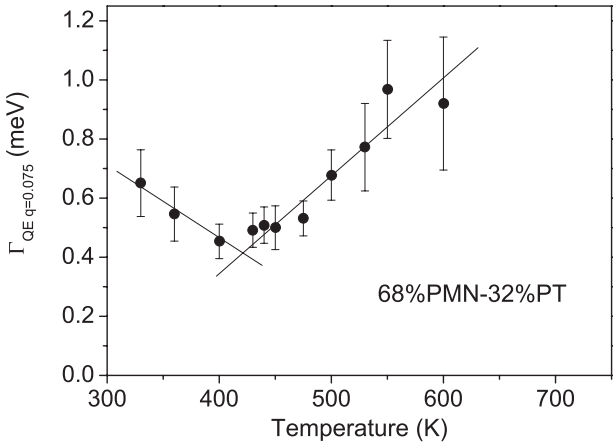

Figure 11. The temperature dependence of the damping of the quasi-elastic scattering as measured at (1, 1, 0.075). The fits are to two linear power laws.

results were deduced from the scattering at (2, 2, 0.075). The energy width of the quasi-elastic scattering steadily decreases from about 1 meV just below 700 K to a minimum energy width of just below 0.5 meV at 430 K. On further cooling the energy width tends to increase as shown in figure 11. These results are similar to those obtained in PMN, except that the energy width of the scattering steadily decreases on cooling in PMN in contrast to the increase observed in the doped material below 420 K.

A detailed study of the shape of the quasi-elastic scattering was made at both 430 and 475 K by measuring a series of scans with the wavevector transfer along the (1, 1, q) direction with the component q varying between 0.035 and 0.125 rlu. The results of the fitting to the coupled-mode model with an additional quasi-elastic component are given in figures 12–14. Figure 12 shows the wavevector dependence of the quasi-elastic scattering intensity at 475 K, and it is clearly peaked at small wavevectors. A fit to a Lorentzian curve gives an inverse correlation length of about 0.039 rlu. Figure 13 shows the width compared with that observed

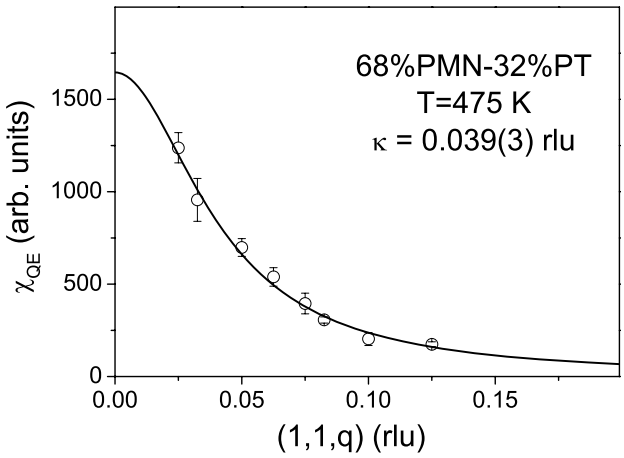

Figure 12. The wavevector dependence of the susceptibility of the quasi-elastic scattering measured close to the (110) Bragg reflection.

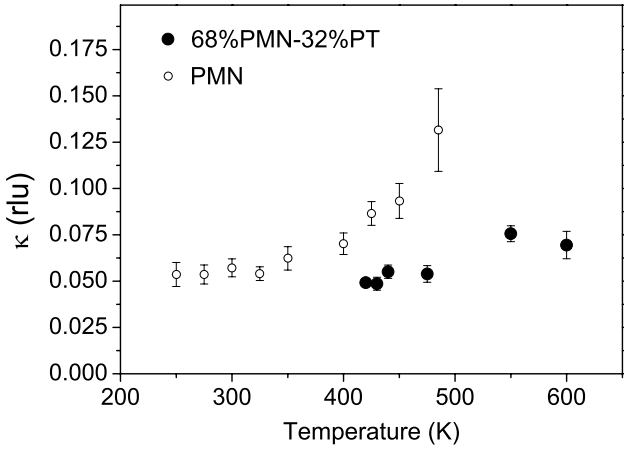

Figure 13. The width in reciprocal space of the quasi-elastic scattering as a function of temperature. The measurements were made near the (110) Bragg reflection, and the results for 0.68PMN–0.32PT are compared with those from PMN.

in PMN. The magnitudes are similar, although there is less temperature dependence for the present sample than for PMN. Figure 14 shows the increasing width in the quasi-elastic energy when the wavevector is increased. The results are consistent with fits to

$$\Gamma(q) = \Gamma_0 + D_{\mathrm{QE}} q^2 \tag{6}$$

with $\Gamma_0 = 0.19 \pm 0.09$ and 0.26 ± 0.06 meV at 430 and 475 K, respectively, while $D_{\mathrm{QE}} = 64 \pm 23$ and 54 ± 12 meV/q^2.

3.4. Central peak intensity

The spectra shown in figure 7 also show that there is considerable scattering from an elastic resolution-limited peak known as the central peak, CP. The temperature dependence of the scattering intensity measured at a wavevector transfer of (1, 1, 0.075) is shown in figure 15.

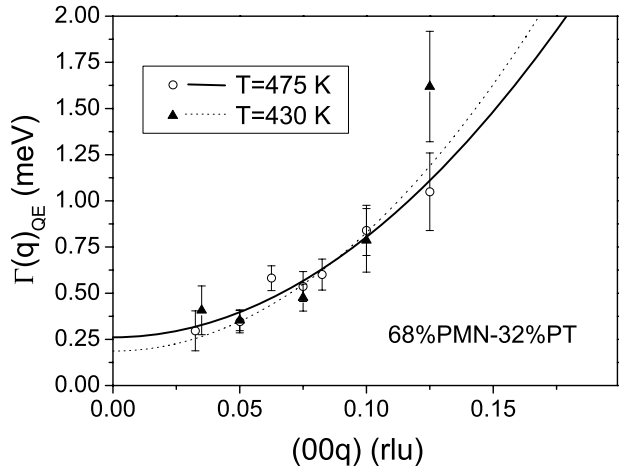

Figure 14. The wavevector dependence of the damping of the quasi-elastic scattering measured in the vicinity of the (110) Bragg reflection.

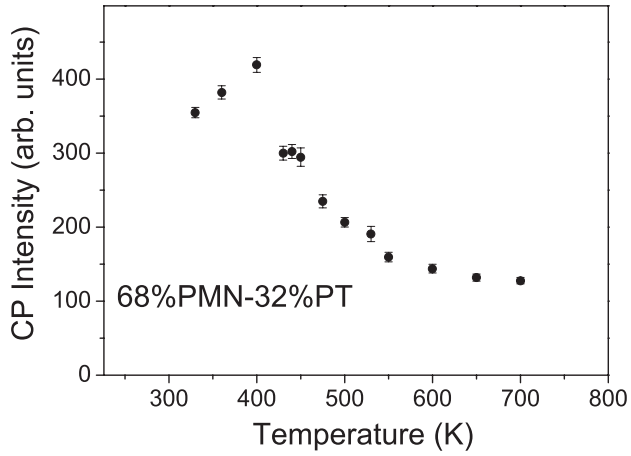

Figure 15. The temperature dependence of the central peak (energy resolution-limited peak) as a function of temperature. The results are taken from the data at a wavevector transfer of (1, 1, 0.075).

The intensity is almost independent of temperature, above a temperature of 550 K, at a value presumably given by the defect scattering and the incoherent scattering. This scattering away from the Bragg reflections has a maximum at a temperature of about 400 K and then decreases on further cooling. Unfortunately we were unable to obtain a precise wavevector dependence of this scattering due to the relatively low intensity of the CP as compared to both the quasi-elastic scattering and the Bragg peak.

4. Discussion

PMN doped with 32% of PT has been studied with high-resolution cold-neutron inelastic scattering techniques. The results show that at a high temperature there is a conventional strong coupling between the TA mode and the lowest-frequency TO mode that can be analysed with

the same formalism as was applied to PMN. On cooling the sample the high resolution of the experiments enabled us to observe both a QE peak and a resolution-limited CP in addition to the scattering from the TO and TA phonon modes. The QE peak has a broad maximum at approximately the temperature of the ferroelectric phase transition where both the damping and the inverse correlation length have minima. The intensity of the CP also has a weak maximum at about the same temperature. At the temperature where the quasi-elastic scattering appears the damping of the TO phonon starts to increase and the stiffness of the TO branch indicates a slight maximum. This may be a consequence of the scattering by the dynamic nanoregions.

Above the ferroelectric phase transition temperature these results are similar to those obtained from PMN except for the fact that the central peak is weaker in intensity and persists for temperatures well above the maximum of the dielectric susceptibility. Below the ferroelectric phase transition temperature both the quasi-elastic peak and the central peak decrease in intensity, whereas for PMN the central peak continued to increase in intensity down to the lowest temperature [11]. This is consistent with the structure of PMN consisting of a large number of randomly oriented polar nanoregions, whereas in PMN doped with 32% of PT the polar nanoregions all tend to become aligned. The crystal is then ferroelectric with the different nanoregions contributing to the uniform ferroelectric moment in a particular direction. This is possibly surprising because this doped sample is very close to the concentration at which the cubic anisotropy is very small, and we would expect there was little preference for any particular domain orientation. It must, however, be the case that the tendency to produce long-range order is larger than the tendency to produce disorder and static frozen polar nanoregions. In terms of the random-field model that we used to explain our PMN results [11], the random fields do not produce long-range order, but they do give rise to dynamic polar nanoregions, and these produce the quasi-elastic scattering. We then suggested that in PMN there was a transition to a state which was cubic in symmetry rather than having isotropic symmetry and in which the nanoregions became static. This was inferred from the temperature dependence of the central peak for which the intensity was large below the temperature of the maximum of the susceptibility of the quasi-elastic scattering, and further, the central peak was approximately constant below ∼150 K, where the quasi-elastic component disappeared. Much the same behaviour seems to occur in the doped sample, except that static long-range ordered ferroelectricity replaces the static random cubic phase in PMN. This is shown by the increase in the intensity of the central peak when approaching T_c from the paraelectric state and by the decrease of this scattering below a temperature of 400 K.

It is of interest to compare our results with those of Stock *et al* [23], who used a crystal with 0.4PMN–0.6PT, and of Koo *et al* [24], who have studied a sample of 0.8PMN–0.2PT. Both groups used thermal neutron scattering with a scattered neutron energy of 14.8 meV. The sample with 0.4PMN–0.6PT is paraelectric above a temperature of 550 K and on cooling distorts to a long-range ordered tetragonal ferroelectric structure. In this material the damping of the transverse acoustic phonons was found to be small. Nevertheless the lowest transverse optic mode was soft below T_c and exhibited the waterfall effect. There was no quasi-elastic scattering measured which could be identified with polar nanoregions. On the other hand, weak diffuse scattering was observed. We conclude that in this material there is less disorder and the ferroelectric transition temperature has increased up to and possibly above the Burns temperature. There is then a much smaller temperature region for which the polar nanoregions can be observed if at all. The neutron scattering results of Koo *et al* [24] were not able to separate out the quasi-elastic and central peak components of the scattering but their measurements do suggest that a cold neutron experiment on this material would give results that are intermediate between those obtained from PMN and those obtained from 0.68PMN–0.32PT.

In conclusion, we consider that our results on 0.68PMN–0.32PT taken together with those obtained on PMN [11], 0.4PMN–0.6PT [23] and 0.8PMN–0.2PT [24] enable us to have a consistent phenomenological picture. At the PMN end of the phase diagram there is a strong coupling between the optic and acoustic transverse modes, and this gives rise to the different line-shapes of the scattering in different Brillouin zones. At low energies and below the Burns temperature there is quasi-elastic scattering from the polar nanoregions which are in dynamic motion as predicted by the isotropic random field model [13]. At lower temperatures either there is a ferroelectric transition to long-range order as for concentrations near 32% of PT or the system fails to obtain long-range order when the structure consists of static polar nanoregions as found for PMN. Random fields have been shown to play a crucial role in these relaxor ferroelectrics and we suggest that cubic anisotropy should also be considered to understand these results in quantitative detail.

Acknowledgments

The experiments were performed at the spallation neutron source SINQ, Paul Scherrer Institut, Villigen (Switzerland). This research was partially supported by the Grant-in-Aid for Scientific Research (A), 16204032 under MEXT, Japan and by RFBR grant 05-02-17822.

References

[1] Smolenskii G A, Bokov V A, Isupov V A, Krainik N N, Pasynkov R E and Sokolov A I 1984 *Ferroelectrics and Related Materials* (New York: Gordon and Breach)
[2] Cross L E 1987 *Ferroelectrics* **76** 241
[3] Westphal V, Kleeman W and Glinchuk M D 1992 *Phys. Rev. Lett.* **68** 847
[4] Viehland D, Jang S J, Cross L E and Wuttig M 1992 *Phys. Rev.* B **46** 8003
[5] Blinc R, Dolinsek J, Gregorovic A, Zalar B, Filipic C, Kutnjak Z, Levstik A and Pirc R 1999 *Phys. Rev. Lett.* **83** 424
[6] de Mathan N, Husson E, Calvarin G, Gavarri J R, Hewat A R and Morell A 1991 *J. Phys.: Condens. Matter* **3** 8159
[7] Burns G and Scott B A 1973 *Solid State Commun.* **13** 423
[8] Vakhrushev S B, Kvyatkovsky B E, Nabereznov A A, Okuneva N M and Toperverg B P 1989 *Physica* B **156/157** 90
[9] Gvasaliya S N, Lushnikov S G and Roessli B 2004 *Phys. Rev.* B **69** 092105
[10] Wakimoto S, Stock C, Ye Z G, Chen W, Gehring P M and Shirane G 2002 *Phys. Rev.* B **66** 224102
[11] Gvasaliya S N, Roessli B, Cowley R A, Hubert P and Lushnikov S G 2005 *J. Phys.: Condens. Matter* **17** 4343
[12] Stock C, Birgeneau R J, Wakimoto S, Gardiner J, Chen W, Ye Z G and Shirane G 2004 *Phys. Rev.* B **69** 094104
[13] Imry Y and Ma S K 1975 *Phys. Rev. Lett.* **35** 1399
[14] Birgeneau R J, Cowley R A, Shirane G and Yoshizawa H 1985 *Phys. Rev. Lett.* **54** 2147
[15] Shirane G, Axe J D, Harada J and Remeika J P 1970 *Phys. Rev.* B **2** 155
[16] Noheda B, Zhong Z, Cox D E, Shirane G, Park S E and Rehrig P 2002 *Phys. Rev.* B 224101
[17] Ye Z G, Bing Y, Gao J, Bokov A A, Stephens P, Noheda B and Shirane G 2003 *Phys. Rev.* B **67** 104104
[18] Zekria D and Glazer A M 2004 *J. Appl. Crystallogr.* **37** 143
[19] Shuvaeva V A, Glazer A M and Zekria D 2005 *J. Phys.: Condens. Matter* **17** 5709
[20] Singh A K, Pandey D and Zaharko O 2006 *Phys. Rev.* B **74** 024101
[21] Devonshire A F 1949 *Phil. Mag.* **40** 1040
[22] Vanderbilt D and Cohen M H 2001 *Phys. Rev.* B **63** 094108
[23] Stock C, Ellis D, Swainson I P, Xu G, Hiraka H, Luo H, Zhao X, Viehland D, Birgeneau R J and Shirane G 2006 *Phys. Rev.* B **73** 064107
[24] Koo T Y, Gehring P M, Shirane G, Kiryukhin V, Lee S-G and Cheong S-W 2002 *Phys. Rev.* B **65** 144113
[25] Semadeni F, Roessli B and Boeni P 2001 *Physica* B **297** 152
[26] Fischer W E 1997 *Physica* B **234–236** 1202